Gallery of Fluid Motion

Turbulence through sustained vortex ring collisions

Takumi Matsuzawa,[1] Noah P. Mitchell,[1,*] Stéphane Perrard,[1,†] and William T. M. Irvine[2]
[1]*James Franck Institute and Department of Physics, University of Chicago, Chicago, Illinois 60637, USA*
[2]*Enrico Fermi Institute, University of Chicago, Chicago, Illinois 60637, USA*

(Received 24 May 2023; published 16 November 2023)

This paper is associated with a video winner of a 2022 American Physical Society's Division of Fluid Dynamics (DFD) Gallery of Fluid Motion Award for work presented at the DFD Gallery of Fluid Motion. The original video is available online at the Gallery of Fluid Motion, https://doi.org/10.1103/APS.DFD.2022.GFM.V0008

DOI: 10.1103/PhysRevFluids.8.110507

Understanding and controlling turbulence has long been a challenging task [1–3]. A plethora of experimental methods have been developed to reveal its statistical and structural properties as well as its onset. In all cases, however, the material boundaries of the experimental apparatus obscure what the turbulence has been fed, and how it would freely evolve. Can turbulence be confined and held in place, as an isolated cloud in a tank? Being able to create such a state would enable us to ask questions that were challenging to address before. Is there more than one type of turbulence [4] depending on its global input? How are the inviscid conserved quantities (energy, linear impulse, angular impulse, and helicity [5]) transported across the turbulent/nonturbulent interface? Helicity is a topological invariant that characterizes knottedness and linkage of vortex lines of a flow, and constrains fluid motion. How does energy cascade in the presence of helicity? To address this gap in experimental turbulence research, we set out to build and sustain an isolated blob of turbulence, far away from boundaries.

To this end, vortex rings [6,7] is an ideal candidate to build and manipulate the turbulent state. A vortex ring can be readily generated in the laboratory by impulsively drawing water through an orifice. This simple mechanism allows vortex rings to be widely formed in nature from fish wakes [8] to volcanic eruptions [9], as well as in the left ventricle of the human heart [10]. The formation process comes about through a subtle combination of inertial and viscous dynamics, including boundary layer separation, vortex sheet roll up, and viscous entrainment. In our experiments, vortex rings are generated at the orifices placed at the corners of a cubic chamber as a piston, attached on the top face, drawing water into the chamber. Once formed, a vortex loop can travel far away from boundaries, carrying vorticity and the associated inviscid invariants (circulation, energy, linear impulse, angular impulse, and helicity). Moreover, its properties can be fully measured, and tuned via the orifice geometry and the stroke speed.

*Present address: Kavli Institute for Theoretical Physics and Department of Physics, University of California, Santa Barbara, California, USA.
†Present address: PMMH, CNRS, ESPCI Paris, Université PSL, Sorbonne Université, Université de Paris, 7, quai Saint Bernard, 75005, Paris, France.

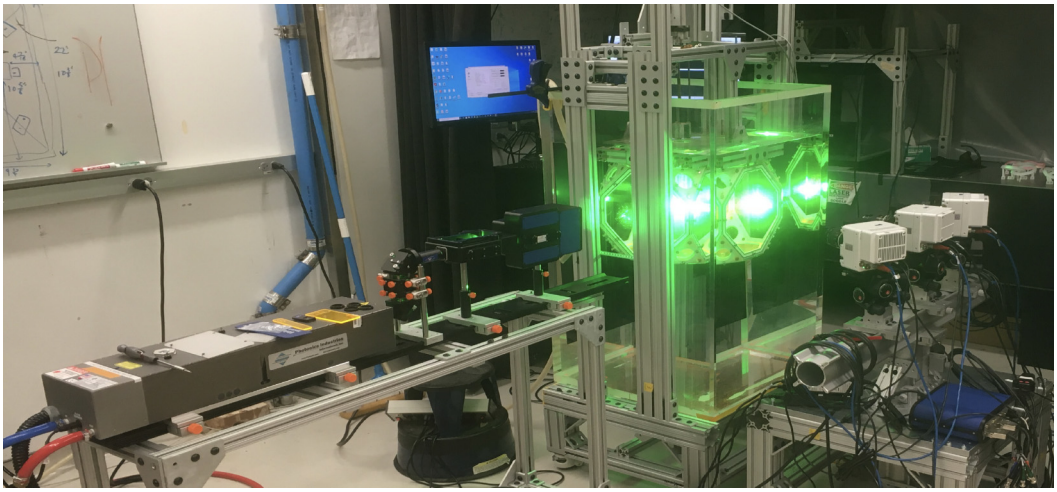

FIG. 1. The 3D PTV setup. (Left) A Nd:YDF, pulsed laser and two cylindrical lenses are used to create an illuminated region in the chamber. (Middle) The 3D-printed, standard chamber is fixed in a water tank. (Right) Multiple (up to four) high-speed cameras are mounted on the mobile cart.

Combining vortices to build turbulence is, however, no simple feat. As shown in iconic vortex collision experiments [11,12], two vortex rings, fired toward each other, can multiply into a series of smaller rings through a process called "vortex reconnection" [13]. While this minimal system already exhibits a cascading behavior of turbulence [14], it also highlights the tendency of vortices to divide and redirect. Early on in our video, we present experimental footage of multiple vortex ring collisions in our tank, as well as the simulations based on the Gross-Pitaevskii equation. These experiments showcase the recombination of vortices and their subsequent escape from the collisions, propagating outward.

To better visualize these complex and exquisite phenomena, we perform 3D particle tracking velocimetry (3D PTV) as illustrated in Fig. 1. The experimental system consists of multiple (up to four) high-speed cameras, a pulsed laser, a timing box, and a set of cylindrical lenses. By using the shake-the-box particle tracking algorithm [15], we track over 100 000 fluorescent particles in the illuminated volume, and identify the particles transported by vortex rings based on their detected positions and speeds. The registered trajectories are then reconstructed using a 3D rendering software (Houdini, SideFX). Inspired by the iconic head-on collision experiment, we color the particle tracks by their associations to the vortex rings that initially transport them. The resulting visualization illustrates the entirety of the reconnection process: eight vortex rings collide [Fig. 2(a)], reconnect, and form six outgoing vortex rings. As illustrated in Fig. 2(b), each of these outgoing rings is built out of four sections that each carries particles from distinct parental vortex rings.

At odds with this tendency of vorticity to escape, we discovered that firing vortex rings repeatedly results in more complex vortex reconnections, and can generate a steady, isolated blob of turbulence. What suppresses the escaping behavior of the vortex loops? The most basic argument is given by geometry: the outgoing rings collide with the incoming rings above a certain injection frequency. With a small number of injected vortex loops ($n = 2$ or 4), the outgoing loops travel in the directions perpendicular to the incoming ones, making it difficult to confine vorticity to form a blob. When eight vortex loops repeatedly collide, the outgoing vortex loops do not travel completely perpendicular to the incoming directions, allowing them to interact. A visualization of coherent vorticity supports this hypothesis (see Fig. 28 of the SM in [16]). Time-averaging energy density reveals the presence of an energetic blob with eight pillars branching out of it [Fig. 3(a)]. The flow inside the blob is in stark contrast with the surroundings which remain relatively quiescent.

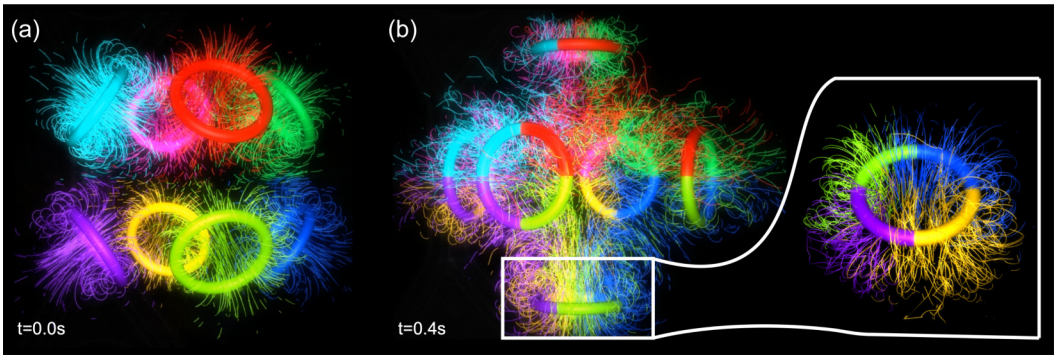

FIG. 2. Visualization of a single-shot collision of eight identical vortex rings using tracer trajectories at an initial Reynolds number of approximately 1000. (a) Tracer trajectories of particles transported by the vortex rings before the collision ($t = 0$ s), with colors assigned by their association with the rings. (b) Vortex reconnection process generates six outgoing rings after the collision ($t = 0.4$ s), with an inset close-up view of a secondary ring consisting of quarters of four parental rings. To improve visibility, we superimposed the tracer trajectories obtained from five different runs. The tori are a guide to the eye. Their diameters are 15 mm. https://doi.org/10.1103/APS.DFD.2022.GFM.V0008

This environment is punctuated by the passage of the incoming coherent vortex rings, with their paths clearly visible in the energy of the mean flow displayed as a yellow cloud in Fig. 3(a). By contrast, the flow inside the blob is dominated by fluctuations as illustrated by a blue cloud in Fig. 3(a). When tracer particles travel through this fluctuating region, their trajectories are complex and unpredictable [Fig. 3(b)] compared to the case when the coherent vortex reconnection takes

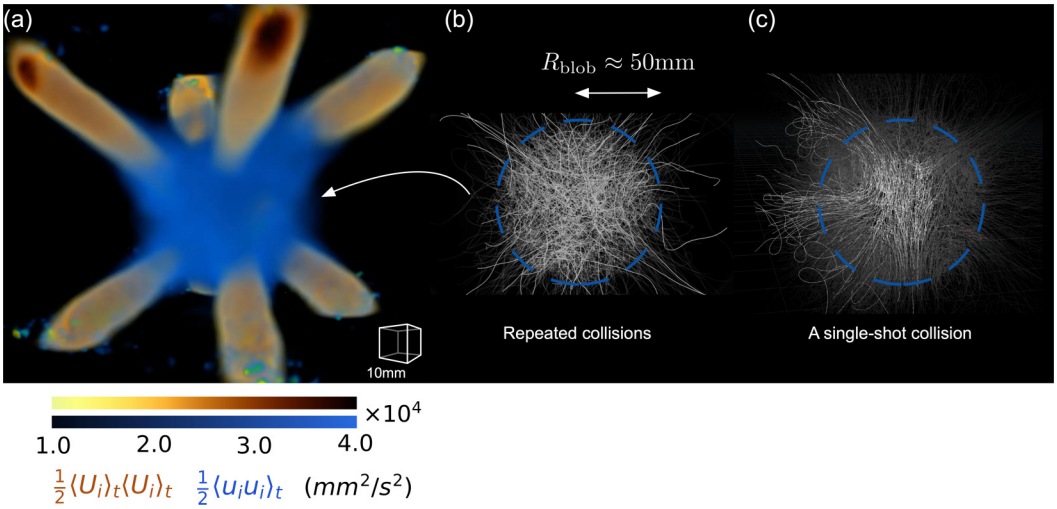

FIG. 3. Repeated collision of eight vortex rings forms an isolated blob of turbulence. (a) The decomposition of the energy density into (time-averaged) mean flow (yellow) and fluctuating (blue) parts illustrates the formation of confined turbulence. (b) Highly irregular tracer trajectories are observed inside the turbulent blob. (c) Coherent tracer trajectories are observed when only a single set of vortex rings collides. For both (b) and (c), only a fraction of the trajectories are highlighted for clarity. https://doi.org/10.1103/APS.DFD.2022.GFM.V0008

place [Fig. 3(c)]. Our energy spectra and structure function, a measure of the velocity fluctuations at different spatial scales, support the notion that the flow inside the blob is turbulent.

This decomposition of the flow into the mean and the fluctuations presents a picture in which an isolated blob of turbulence is fed, and controlled by the injected vortex loops. Our analysis of the energy budget supports this view. Moreover, the injected power determines the smallest scale of turbulent motions, Kolmogorov scale. The size of the blob is set by the radius of the injected vortex ring. Hence, the range of the spatial scales is fully controlled by the injected vortex rings. Crucially, all of the inviscid invariants of the blob (energy, linear impulse, angular impulse, and helicity) are set by those of a vortex loop. Similarly, all of the inviscid invariants of the blob are set by those of the vortex loops. To be able to tune these invariants required invention of an orifice that could produce helical vortex loops: helical loops carry nontrivial amounts of all the inviscid invariants; combining left- and right-handed sets enabled us to inject any combination of energy, impulse, angular impulse, and helicity. Our 3D PTV measurements confirm the transfer of helicity from a coherent to a turbulent state.

Our experiments show that, by combining vortex loops, turbulence can be localized, positioned, and controlled. The findings enable enhanced mixing away from the boundaries, and translate local turbulence to a targeted position. Our highly tunable turbulent blob offers a playground to investigate fundamental studies on inhomogeneous turbulence, such as the decay of turbulence without interference from boundaries, and transport at the turbulent/nonturbulent interface. With controlled injection of inviscid invariants, our approach enables to create various types of turbulence such as Saffman turbulence (nonzero linear impulse and zero helicity), Batchelor turbulence (negligible linear impulse and zero helicity), and helical turbulence (nonzero helicity). Because energy decays with different power laws for the Saffman and Batchelor turbulence, exploring the difference may result in an effective method to speed up turbulence decay. An immediate next step is to investigate how turbulence evolves freely in a quiescent environment. For the complete description of the achieved flow, the authors invite readers to see Ref. [16].

This work was supported by the Army Research Office through No. W911NF-17-S-0002, No. W911NF-18-1-0046, and No. W911NF-20-1-0117, a 2021 Brown Investigator Award from the Brown Science Foundation. We also acknowledge LaVision Inc. for their support on the particle image velocimetry and the particle tracking velocimetry, SideFX, and Object Research Systems for granting software licenses (Houdini and Dragonfly, respectively) to visualize flows. The Chicago MRSEC is gratefully acknowledged for access to its shared experimental facilities (US NSF Grant DMR2011854). For access to computational resources, we thank the University of Chicago's Research Computing Center and the University of Chicago's GPU-based high-performance computing system (NSF DMR-1828629).

[1] P. Davidson, *Turbulence: An Introduction for Scientists and Engineers* (Oxford University Press, Oxford, 2015).
[2] S. B. Pope, *Turbulent Flows* (Cambridge University Press, Cambridge, New York, 2000).
[3] J. Lumley and P. Blossey, Control of turbulence, Annu. Rev. Fluid Mech. **30**, 311 (1998).
[4] P.-Å. Krogstad and P. Davidson, Is grid turbulence saffman turbulence? J. Fluid Mech. **642**, 373 (2010).
[5] H. K. Moffatt, Helicity and singular structures in fluid dynamics, Proc. Natl. Acad. Sci. **111**, 3663 (2014).
[6] D. G. Akhmetov, *Vortex Rings* (Springer Berlin, Heidelberg, 2009).
[7] K. Shariff and A. Leonard, Vortex rings, Annu. Rev. Fluid Mech. **24**, 235 (1992).
[8] E. G. Drucker and G. V. Lauder, Locomotor forces on a swimming fish: Three-dimensional vortex wake dynamics quantified using digital particle image velocimetry, J. Exp. Biol. **202**, 2393 (1999).
[9] F. Pulvirenti, S. Scollo, C. Ferlito, and F. M. Schwandner, Dynamics of volcanic vortex rings, Sci. Rep. **13**, 2369 (2023).

[10] J. O. Dabiri, Optimal vortex formation as a unifying principle in biological propulsion, Annu. Rev. Fluid Mech. **41**, 17 (2009).
[11] Y. Oshima, Head-on Collision of two vortex rings, J. Phys. Soc. Jpn. **44**, 328 (1978).
[12] T. Lim and T. Nickels, Instability and reconnection in the head-on collision of two vortex rings, Nature (London) **357**, 225 (1992).
[13] S. Kida and M. Takaoka, Vortex reconnection, Annu. Rev. Fluid Mech. **26**, 169 (1994).
[14] R. McKeown, R. Ostilla-Mónico, A. Pumir, M. P. Brenner, and S. M. Rubinstein, Turbulence generation through an iterative cascade of the elliptical instability, Sci. Adv. **6**, eaaz2717 (2020).
[15] D. Schanz, S. Gesemann, and A. Schröder, Shake-The-Box: Lagrangian particle tracking at high particle image densities, Exp. Fluids **57**, 70 (2016).
[16] T. Matsuzawa, N. P. Mitchell, S. Perrard, and W. T. M. Irvine, Creation of an isolated turbulent blob fed by vortex rings, Nat. Phys. **19**, 1193 (2023).